Bioprocess Biosyst Eng (2018) 41:21–30
https://doi.org/10.1007/s00449-017-1840-9

RESEARCH PAPER

Green approach for synthesis of zinc oxide nanoparticles from *Andrographis paniculata* leaf extract and evaluation of their antioxidant, anti-diabetic, and anti-inflammatory activities

Govindasamy Rajakumar[1] · Muthu Thiruvengadam[1] · Govindarasu Mydhili[2] · Thandapani Gomathi[3] · Ill-Min Chung[1]

Received: 6 June 2017 / Accepted: 8 September 2017 / Published online: 15 September 2017

Abstract Bio-mediated synthesis of zinc oxide nanoparticles (ZnO NPs) was carried out by utilizing the reducing and capping potential of *Andrographis paniculata* leaf extract. The capped ZnO NPs were characterized using UV–Vis, XRD, FTIR, SEM, TEM and SAED analyses. FTIR analysis suggested the role of phenolic compounds, terpenoids, and proteins of *A. paniculata* leaf extract, in nucleation and stability of ZnO NPs. XRD pattern compared with the standard confirmed spectrum of zinc oxide particles formed in the present experiments were in the form of nanocrystals, as evidenced by the peaks at 2θ values. SEM and TEM analysis of ZnO NPs reveals those spherical and hexagonal shapes and the sizes at the range of 96–115 and 57 ± 0.3 nm, respectively. The synthesized nanoparticles possess strong biological activities regarding anti-oxidant, anti-diabetic, and anti-inflammatory potentials which could be utilized in various biological applications by the cosmetic, food and biomedical industries.

Keywords Zinc oxide nanoparticles · *Andrographis paniculata* · Characterization · Antioxidant · Antidiabetic

✉ Thandapani Gomathi
drgoms1@gmail.com; chemist.goms@gmail.com

✉ Ill-Min Chung
imcim@konkuk.ac.kr

[1] Department of Applied Bioscience, College of Life and Environmental Science, Konkuk University, Seoul, South Korea

[2] Department of Biochemistry, Periyar University, Salem, Tamil Nadu 636011, India

[3] Department of Chemistry, D.K.M. College for Women, Vellore, Tamil Nadu, India

Introduction

Nanobiotechnology is an important and emerging technical tool for the development of an eco-friendly and reliable methodology for the synthesis of nanoscale materials using biological sources [1]. Recently, bionanotechnology is a rapidly advancing area of scientific and technological opportunity that applies the tools and process of nano/microfabrication to build devices for studying biosystems. It concerned with molecular scale properties such as size, shape, and surface morphology and applications of nanostructures and its interface between the chemical, biological, physical, optical, and electronic properties of nano materials [2]. Owing to the medical and pharmaceutical applications, nanoparticles (NPs) of noble metals, such as gold, silver, platinum, and zinc oxide are widely practiced [3]. Nanoparticles produced by plants are more stable and more varied in shape and size in comparison with those produced by other organisms [4]. Among metal oxide nanoparticles, zinc oxide (ZnO) has received much attention in the recent past. ZnO nanostructures are the forefront of research due to their unique properties and wide applications [5].

In particular, utilization of medicinal plant extracts as potential reducing and stabilization agents to synthesis ZnO nanostructures attainment many advantages over conventional physical and highly toxic chemical methods [6]. The advantages of nanostructured ZnO particles over other metal nanoparticles are due to their lower cost, UV blocking properties, high catalytic activity, large surface area, white appearance and their remarkable applications in the field of medicine, environmental remediation, antimicrobial activity and agriculture [7–9]. Several recent plants have been successfully employed for efficient and rapid extracellular biosynthesis of ZnO NPs. For examples,

Pongamia pinnata [10], *Vitex trifolia* [11], *Ficus benghalensis* [12], *Punica granatum* [13], *Trifolium pratense* [14], *Hibiscus subdariffa* [15] and *Couroupita guianensis* Aubl. [16].

Andrographis paniculata (Burm.f.) Wall. ex Nees (*A. paniculata*) is an important medicinal plant which belongs to the family Acanthaceae and used as a traditional herbal medicine in Bangladesh, China, Hong Kong, India, Pakistan, Philippines, Malaysia, Indonesia, and Thailand [17, 18]. *A. paniculata* has been reported to have a broad range of pharmacological effects including anti-cancer [19, 20], anti-diarrheal [21], anti-hepatitis [22], anti-HIV [23], anti-hyperglycemic [24], anti-inflammatory [25], antimicrobial, anti-malarial [26], anti-oxidant [27], cardiovascular [28], cytotoxic [23], hepatoprotective [29] immunostimulatory [30], and sexual dysfunctions [31]. Aqueous extract of *A. paniculata* was more potent than ethanolic extract in anti-oxidant activities; compared with andrographolide, the aqueous extract also possessed potent anti-oedema and analgesic activities [32]. Thus, in the present study, ZnO NPs were aimed to prepare through green synthesis using the leaf of *A. paniculata*, which include low cost, nontoxicity, and the ability to prepare compounds with varying morphologies having different prosperities by utilizing reducing and capping potential.

Materials and methods

Preparation of *A. paniculata* leaf extract

Fresh leaves of *A. paniculata* were collected from Vellore, Vellore district, Tamil Nadu, India, washed thoroughly with double distilled water and incised into small pieces. From this 10 g were weighed and transferred into a 250-mL beaker containing 100 mL of double distilled water, mixed well and boiled for 2 min. The extract obtained was filtered through Whatman no. 1 filter paper, and the filtrate was collected in 250-mL Erlenmeyer flask and stored at 4 °C for further use.

Synthesis of ZnO NPs

Biosynthesis of ZnO NPs was carried out according to the method of Murali et al. [33] with modifications. About, 10 g of leaf material was extracted with 100 mL of sterile distilled water and filtered through Whatman no. 1 filter paper. The plant extract (about 20 mL) was boiled (60–80 °C) on a magnetic stirrer. When the temperature of the extract reached 60 °C, 2 g of zinc nitrate hexahydrate [$Zn(NO_3)_2{\cdot}6H_2O$] was added and allowed to boil until the extract became a paste. The collected plant extract was then heated in a furnace at 400 °C for 2 h. The resultant dried material was powdered and stored in an airtight container for further analysis.

Characterization of ZnO NPs

The visual color change observed the preliminary detection for ZnO NPs formation. Reduction of Zn^{2+} in the prepared mixtures was monitored by UV–Vis spectral analysis from 200 to 700 nm using UV–Vis spectrophotometer (Shimadzu, UV 1601). The crystalline structure of the biosynthesized ZnO NPs was investigated by the X-ray diffraction a using X-ray diffractometer (Perkin-Elmer spectrum). XRD spectrum was recorded from 20° to 80° 2θ angles using CuKα radiation operated at 10 kV and 30 mA. FTIR spectra were obtained in the 400–4000^{-1} spectral range with a Perkin-Elmer 1725X FTIR spectrometer using the KBr pellet technique and detect surface functional groups. For FTIR measurements, a small amount of powdered ZnO NPs was placed on round-shaped zinc selenide plate for FTIR spectral analysis. The suspension of ZnO NPs was dried and subjected to SEM–EDS using a JEOL MODEL JSM 6360 SEM. The shape, size, and microstructures of the products obtained were analyzed by transmission electron microscopy (Model JEM 3100 LV, JOEL, USA).

Anti-oxidant activity assays

1-Diphenyl-1-2-picrylhydrazyl (DPPH) scavenging assay

A. paniculata leaf extract and synthesized ZnO NPs were screened for free radical scavenging activity by DPPH method [34]. The scavenging activity on the DPPH radical was determined by measuring the absorbance at 517 nm using a UV-spectrophotometer. Radical scavenging activity was calculated using the formula (Eq. (1)):

$$\%I = \frac{A_{\text{control}} - A_{\text{sample}}}{A_{\text{control}}} \times 100, \quad (1)$$

where $\%I$ is the % of radical scavenging activity, A_{control} is the absorbance of the control sample (DPPH solution without test sample), and A_{sample} is the absorbance of the test sample (DPPH solution with test compound). All tests were performed in triplicate, and the results were averaged.

Reducing power assay

The reducing power was determined according to the method of Oyaizu [35]. Various concentrations of leaf extracts of *A. paniculata* and biosynthesized ZnO NPs were mixed with 2.5 mL of 0.2 M sodium phosphate buffer (pH 6.6) and 2.5 mL of 1% potassium ferricyanide. The mixture was incubated at 50 °C for 20 min. After the addition

of 2.5 mL of 10% trichloroacetic acid (w/v), the mixture was centrifuged at 3000 rpm for 10 min. The upper layer was mixed with 5 mL of deionized water and 1 mL of 0.1% of ferric chloride, and the absorbance was measured at 700 nm. A higher absorbance indicates higher reducing power. ascorbic acid was used as a standard.

Nitric oxide (NO) free radical scavenging activity

Nitric oxide has been involved in a variety of biological functions, including anti-microbial, vascular homeostasis, neurotransmission, and anti-tumor activities. Nitric oxide, generated from sodium nitroprusside, was measured spectrophotometrically by Griess reaction. About 100, 200, 300, 400, and 500 µL (1:1 w/v) concentrations of ZnO NPs previously dissolved in DMSO, as well as ascorbic acid (standard compound), was taken in separated tubes and each tube 2.0 mL of sodium nitroprusside in phosphate buffer saline was added. The solution was incubated at room temperature for 150 min. After incubation, 5 mL of the Griess reagent was added, in each tube including control. Methanol was used as a blank. The absorbance was measured at 546 nm on UV–visible spectrometer [36].

$$\%\,\text{Scavenging reduction} = \frac{T_0 - T}{T_0} \times 100,$$

where T_0 is the absorbance of control and T is the absorbance of the test sample.

Anti-diabetic potential of NPs (α-amylase inhibitory activity)

In brief, 100 µL of different concentrations of the *A. paniculata* leaf extract, $ZnNo_3$, ZnO NPs were allowed to react with 200 µL of the α-amylase enzyme (Hi-media Rm 638) and 100 µL of 2 mM phosphate buffer (pH 6.9). After 20 min incubation, 100 mL of 1% starch solution was added. The same was performed for the control where 200 µL of the enzyme was replaced by the buffer. After incubation for 5 min, 500 µL of dinitro salicylic acid reagent was added to both control and test, and were boiled for 5 min in a water bath. The absorbance was recorded at 540 nm, and the result was interpreted regarding the IC_{50} values (effective concentration showing 50% inhibition activity) [37].

Anti-inflammatory activity of ZnO NPs

The anti-inflammatory activity of the biosynthesized nanoparticles to inhibit protein denaturation was studied through in vitro assay. To 50 µL of different concentrations of the NPs, 5 mL of 0.2% w/v BSA was added and was heated at 72 °C for 5 min and then cooled for 10 min. 5 mL of 0.2% w/v BSA solution with 50 µL water was used as control and Diclofenac (100 µg/mL) in water with 5 mL 0.2% w/v BSA solution was used as a standard. The absorbance was measured at a wavelength of 276 nm [38]. The result was interpreted in terms of the IC_{50} values (effective concentration showing 50% inhibition activity).

Statistical analysis

All experiments were carried out in triplicate and data were analyzed. For the experiments of anti-microbial activity, arithmetic mean values were considered for data analysis. All the statistical analyses were done by SPSS Statistics 18 Release Version 18.0.0, 2009.

Results and discussion

Zinc oxide nanoparticles were synthesized using fresh leaf extract of *A. paniculata*, which were collected from healthy plants, contains the stabilizing agents such as flavanones, terpenoids and reducing sugars as main constituents. Visual examination confirmed the formation of zinc oxide nanoparticles. The color of the mixture was changed from green-yellow to pale white during the reaction, indicating the synthesis of ZnO NPs. It is suggested that the electron rich functional groups of the leaf extract are responsible for the conversion of ZnO NPs. Thus, it is concluded that the *A. paniculata* leaf extract acts as reducing and stabilizing agents for the formation of ZnO NPs.

UV–Vis spectroscopy is the most widely used technique for the structural characterization of nanoparticles. The optical absorption of ZnO NPs dispersed in water was recorded using UV–Vis spectrophotometer (Shimadzu, UV 1601) at room temperature in a quartz cuvette with the path length of 1 cm. The absorbance of the reaction mixture was monitored after 24, 48, 72, 96 and 120 h of reaction. The reduction of zinc nitrate to zinc oxide is monitored by UV–Vis spectrum. All the samples exhibit strong UV absorption spectra with the absorption peak ranging from 358 nm due to its surface plasmon resonance and attain a plateau above 3.3 eV (375 nm) (Fig. 1a). This band is ascribed to excitation of valence electrons of ZnO arranged in the nanoparticles (nanocrystal/nanosphere). The shape of the band was symmetrical, suggesting uniform scattering of spherical shape nanoparticles. According to Gupta et al. [39], the absorption edge systematically shifts to the lower wavelength or higher energy with the decreasing size of the nanoparticle. Thus, there is a strong blue shift in the absorption spectra of the ZnO NPs, indicating that particles must be smaller than the Bohr radius of an exciton which is for ZnO [40]. Similar findings have been documented by

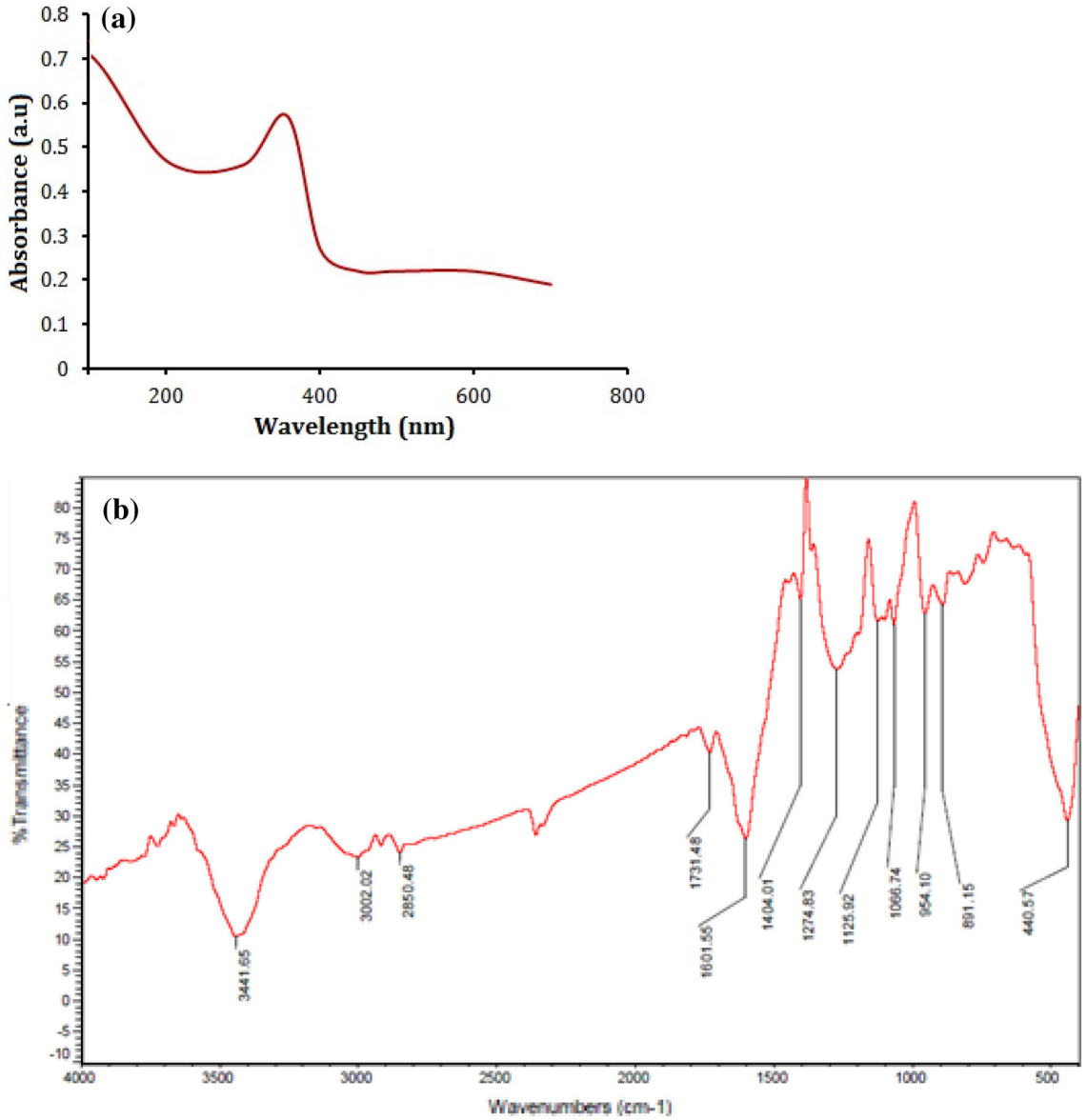

Fig. 1 **a** UV–Vis spectra of biosynthesized ZnO NPs from *A. paniculata*. **b** FTIR spectrum of the synthesized ZnO NPs

Vimala et al. [41] who reported that the absorbance spectra of ZnO NPs were recorded between 330 and 370 nm.

Characterization of ZnO NPs

FTIR gives an impression on the vibrational and rotational modes of the proposition of a molecule, and hence a consistent technique for identification and characterization of the substance. Figure 1b shows the FTIR spectra of ZnO NPs synthesized by the biological method. Possible biomolecules which are responsible for the reduction of ZnO and capping agent of reduced ZnO NPs through distinct bond vibrations peaks stated at bounded wavenumbers were identified [42]. The bands at 3441 cm^{-1} indicate the presence of primary and secondary amines, O–H stretching of alcohols, and intramolecular hydrogen bonding [43]). The bands observed at 3002 and 2850 cm^{-1} have been assigned to asymmetric and symmetric stretching vibrations of C–H. The bands around 1731 and 1601 cm^{-1} are due to the amide I and amide II regions that are characteristics of proteins/enzymes [44]. The spectrum clearly shows ZnO absorption band near 440 cm^{-1} [45, 46]. Also, the intense bands observed at 1404, 1274, 1125, 1066, 954 and 891 1020, 1150 and 1380 cm^{-1} have been assigned to C–H bending, C–N stretching vibrations of aliphatic and aromatic amines, C–O stretching of polysaccharides, alcohols and phenolic groups, respectively. From the FTIR results, it can be concluded that the existence of proteins

and metabolites such as polyphenols, alkaloids carboxylic acid and flavonoids is bound to the surface of ZnO NPs that remained despite repeated washing, and these compounds are responsible for the reduction of zinc ions to ZnO NPs. Furthermore, the stability of the synthesized ZnO NPs is expected to be due to the presence of free amino and carboxylic groups that have interacted with the zinc surface. Moreover, the proteins present in the medium prevent agglomeration and aids in the stabilization by forming a coat, covering the metal nanoparticles [43].

XRD pattern of the prepared ZnO NPs has been shown in Fig. 2. The peak positions with 2θ values are of 31.71°, 34.38°, 36.21°, 45.21°, 47.48°, 56.51°, 62.80°, 67.88° and 69.01° which indexed the planes 100, 002, 110, 102, 110,103, 112 and 201, respectively, reflection lines of hexagonal wurtzite ZnO (JCPDS36-1451) (Fig. 2). All of the diffraction peaks were in adaptation to the hexagonal zinc oxide phase by comparison with the data from cards. The narrow and strong diffraction peaks indicate that the product has a well-crystalline particle structure. The peaks in XRD pattern are derived from their particle size and are by the SEM and TEM observations. No characteristic peaks of any impurities were detected, suggesting that a high quality of ZnO NPs was produced. The crystallite size has been estimated from the XRD pattern using the Scherrer equation (Eq. 1):

$$D = K\lambda/\beta\cos\theta,$$

where $K = 0.9$ is the shape factor, λ is the X-ray wavelength of CuKα radiation (1.54 Å), θ is the Bragg diffraction angle, and β is the full width at half maximum (FWHM) of the respective diffraction peak. Based on the Scherrer equation, the crystallite size of the ZnO NPs was estimated to be 13.8 nm. The image clearly shows the presence of secondary material capping which may be assigned to bio-organic compounds present in the leaf extract that confirm by the observing sharp reflection in the XRD spectrum. The XRD pattern of bio-synthesized ZnO NPs from leaf extract of *Azadirachta indica* stated all the peaks are confirmed ZnO hexagonal phase (wurtzite structure) by comparison with JCPDS card no. 89-7102 [47]

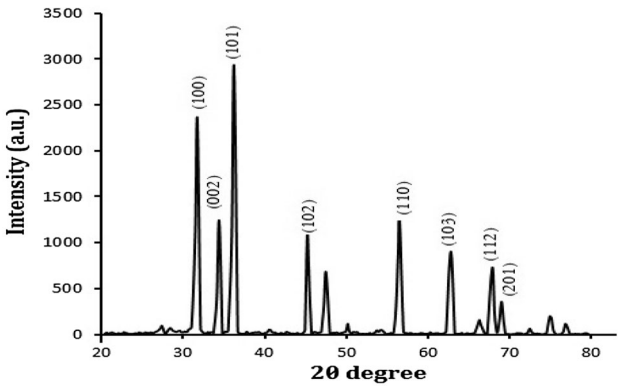

Fig. 2 X-ray diffraction spectra of biosynthesized ZnO NPs from *A. paniculata*

The morphology of the nanostructures obtained from leaves extracts was studied using scanning electron microscopy (SEM). The SEM images of synthesized ZnO NPs exhibit varieties of typical shapes such as spherical and hexagonal nanoparticles. The synthesized ZnO nanoparticles were agglomerated with a particle size ranging from below 96 to 115 nm (Fig. 3a, b). Also, it shows distinguished spherical and hexagonal morphology and generally in random and not uniform, which is very similar to those described in the previous literature [48].

Transmission electron microscopy images of ZnO NPs of different shapes are spherical, oval and hexagonal in size range of 57 ± 0.23 nm (Fig. 4a, b). Especially, the hexagonal (wurtzite) shape is in agreement with the obtained XRD pattern. The images show the presence of zinc oxide nanoparticles agglomeration owing to high surface energy that usually occurs when synthesis is carried

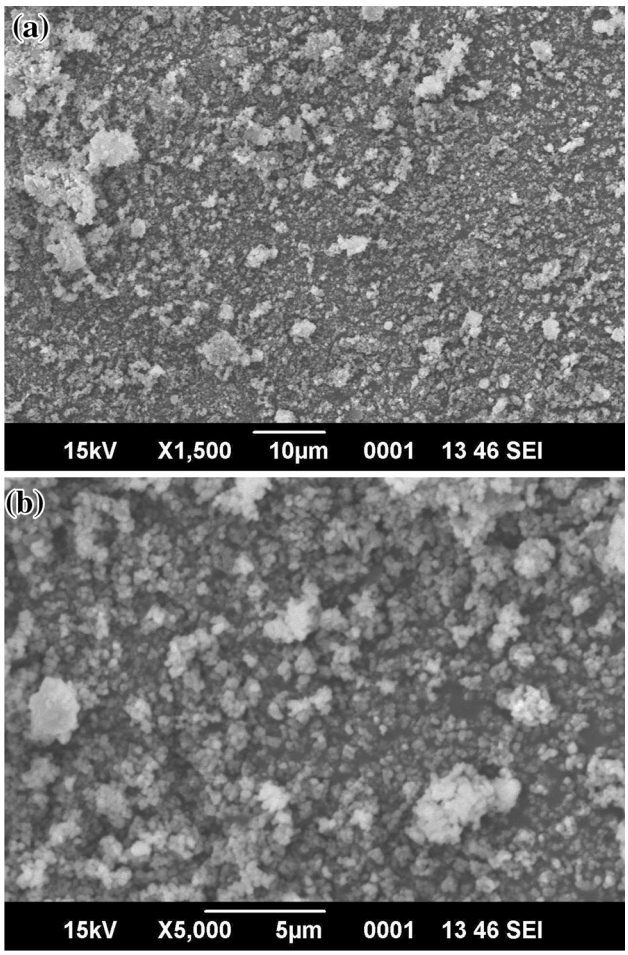

Fig. 3 SEM images of ZnO nanoparticles with various concentrations of *A. paniculata* extract. **a** 10 μm and **b** 5 μm

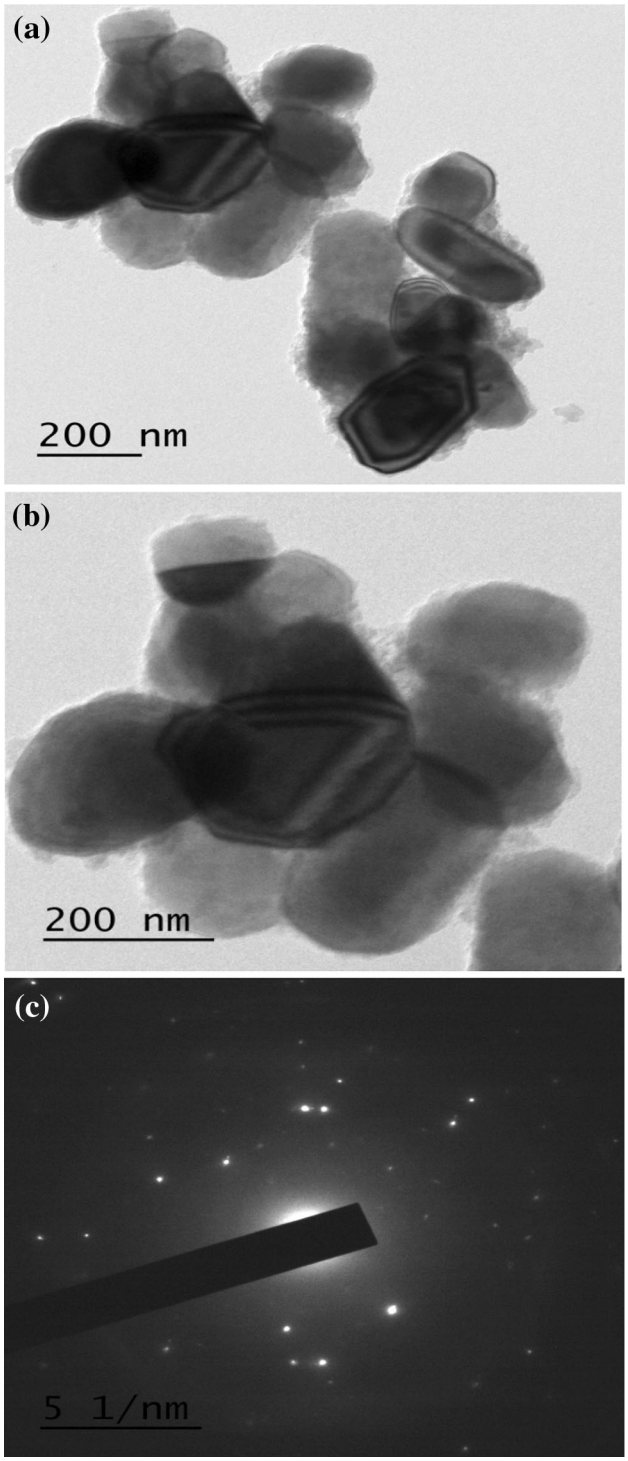

Fig. 4 **a**, **b** TEM image of ZnO NPs synthesized using *A. paniculata* leaf extract. **c** Selected electron diffraction patterns of ZnO NPs

out in an aqueous medium [49]. Owing to the uniform distribution of oxidized metal anions in the three-dimensional polymeric network structure, the agglomeration could be induced by densification resulting in the narrow space between particles [50, 51]. Also, the SAED analysis (Fig. 4c) was proved to be in nanocrystalline nature with SAED rings to be appearing in perfect alignment with the X-ray studies.

The average number of zinc atoms per nanoparticle may be calculated from high-resolution TEM analysis (Liu et al. [59]). The HRTEM images of the synthesized silver nanoparticles show the average particle size of about 57 ± 0.23 nm (D, nm). Assuming a spherical, oval and hexagonal shape, the average number of zinc atoms (N) for each type of nanosphere was calculated by the following equation, where ρ is the density for hcp zinc (7.13 g/cm^3 = 7.13 × 10^{-21} g/nm^3), and M stands for atomic weight of zinc (63.3800 g/mol):

$$N = \frac{\pi}{6}\frac{\rho D^3}{M} N_A = 35.4592 D^3.$$

On applying this above equation, the average number of silver atoms per synthesized nanoparticles was found to be in the range from 6,487,617.529 to 6,646,603.832 atoms.

The free radical scavenging potential of using the DPPH assay is explored for the anti-oxidant activity of the only plant extract and biologically synthesized ZnO NPs. Green synthesized ZnO NPs have almost similar anti-oxidant activity with only plant extract (Fig. 5a). The maximum inhibition (61.32, 57.71%) for biologically synthesized ZnO NPS and plant extract was observed with very low concentration, i.e., 500 µg/mL. Discoloration of violet DPPH to yellow clearly demonstrated the effect of NPs as an antioxidant. Ascorbic acid is used as a standard. During the synthesis of the ZnO NPs, these metabolites are pooled into the NPs. They adsorbed onto the surface of the ZnO NPs. Considering the high surface area to volume ratio, it appears that these ZnO NPs show a high tendency to interact with and reduce DPPH. Therefore, it is possible to propose on Eq. (2):

$$\begin{aligned} \mathrm{H{-}}O\mathrm{{-}(of\ A)} + \mathrm{DPPH} \rightarrow\ & \mathrm{O{=}CH{-}(of\ AA)} \\ & + \mathrm{1{-}1\ diphenyl} \\ & - \mathrm{2\text{-}picrylhydrazine.} \end{aligned} \quad (2)$$

Here hydroxyl of AA quenched the activity of DPPH by donating its electron.

In the functioning of all biosystems, the antioxidants play an important role due to the interaction of biomolecules with molecular oxygen; the free radicals are generated in biological systems [52], which results in the degradation of biomolecules. A crucial role is played by the antioxidants in scavenging these toxic free radicals, thereby terminating the human body's oxidative damage. This study clearly indicates that ZnO NPs synthesized by *Ocimum tenuiflorum* can act as potential antioxidants. Antioxidant activity of ZnO NPs ascribed due to smaller particle grain size and other reason may be a phenomenon of transfer of electron density from oxygen atom to odd

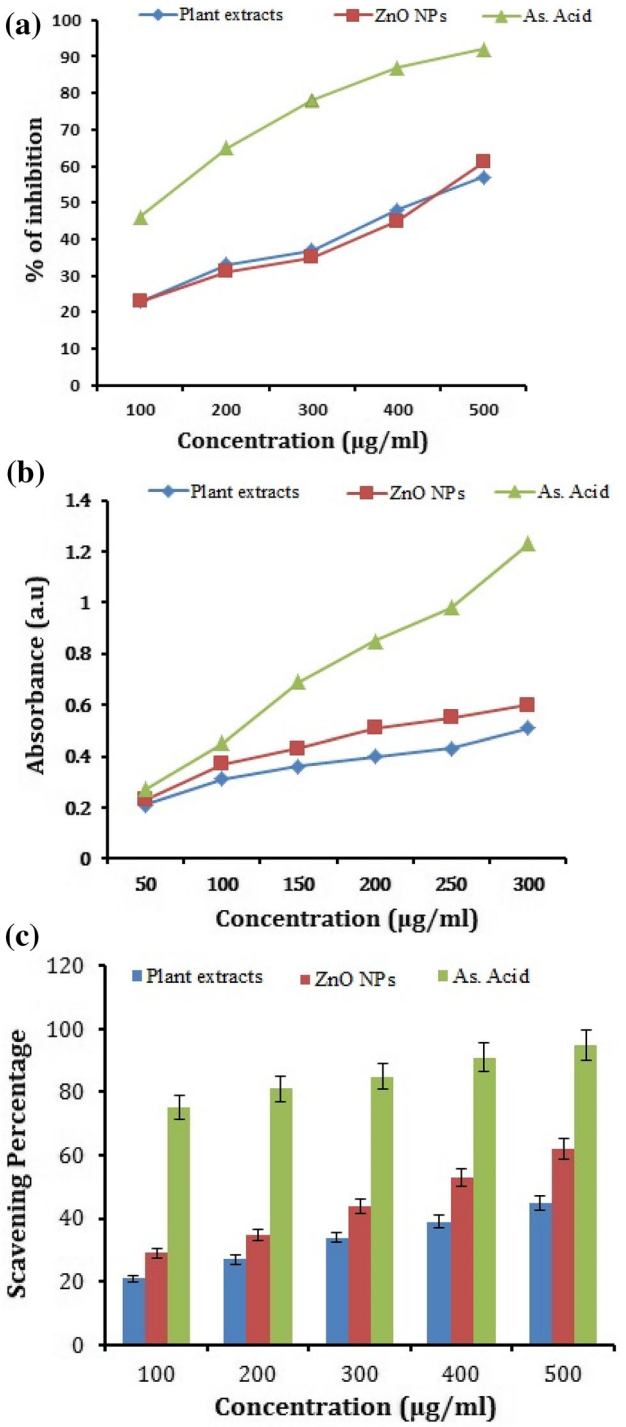

Fig. 5 Anti-oxidant activity of green-synthesized ZnO NPs by **a** DPPH assay, **b** reducing power assay, **c** nitric oxide free radical scavenging activity

electron located at nitrogen atom in DPPH which results in decreasing $n \rightarrow \pi^*$ transition intensity at 517 nm [53].

Reducing power assay indicates that they donate an electron and can reduce the oxidized intermediates of lipid peroxidation process; they act as primary and secondary antioxidants. In the present study, various concentrations of crude extract, biologically synthesized ZnO NPs were taken from 50 to 300 µg and the yellow color of the test solution changes to various shades of green and blue color due to the presence of reducers causing the conversion of Fe^{3+} complex to ferrous form by measuring 700 nm (Fig. 5b). The reducing power was found to be increased with the increase in the concentration of the ZnO NPs, indicating the presence of some compounds in the ZnO NPs acts as both electron donors and could react with free radicals and to terminate free radical chain reactions [54].

The scavenging effect increased with the increasing concentrations of test samples. From the results, the ZnO NPs showed maximum scavenging power of 62% at 500 µL (1:1 w/v) concentrations. Similarly, NO scavenging activity was performed with ZnO NPs and ascorbic acid as standard. The reductive potential of nanoparticle was exhibited on dose dependent manner (Fig. 5c). From the graph, when the concentration increases, the percentage of scavenging is also increasing linearly for tested nanoparticles and ascorbic acid (standard). The results showed the maximum activity of ZnO NPs was 62% at 500 µL (1:1 w/v) concentration. All the graphs were plotted with standard values of ascorbic acid. Antioxidants can also react with NO to form toxic radicals such as hydroxyl radicals by peroxy nitrite [55]. Due to the scavenging power, most of the antioxidants are used in the management of diseases such as neurodegenerative diseases, cancer, AIDS, and so on. Even though the ZnO NPs showed better antioxidant nature, a detailed study on its mechanism is needed for the commercialization of these materials in future.

The synthesized NPs exhibited moderate α-amylase inhibition activity, and the results are presented in terms of the IC_{50} values (Fig. 6a). The IC_{50} values of the ZnO NPs (121.42 µg/mL) were lower than that of the *A. paniculata* leaf extract, $ZnNO_3$, (149.65 and 178.84 µg/mL), respectively, that confirmed that the ZnO NPs displayed better anti-diabetic potential in terms of the α-amylase inhibition activity. Zinc oxide (ZnO) nanoparticles (NPs) have been synthesized using *Hibiscus subdariffa* leaf extract has indicated that small-sized ZnO NPs, stabilized by plant metabolites had better anti-diabetic effect on streptozotocin (STZ)-induced diabetic mice than that of large-sized ZnO particles [15]. ZnO NPs treatment indicates inhibitory effects on glycogenolysis and gluconeogenesis, mechanisms that are active during the fasted state. Interestingly, zinc is reported to regulate glucagon secretion from pancreatic cells [56].

Maximum inhibition activity of 66.78 µg/mL IC_{50} value was observed from the ZnO NPs followed by *A. paniculata* leaf extract, (75.42 µg/mL IC_{50} value), and $ZnNO_3$ (91.33 µg/mL IC_{50} value). Diclofenac, which was taken as the standard reference compound, exhibited 62.55 µg/mL

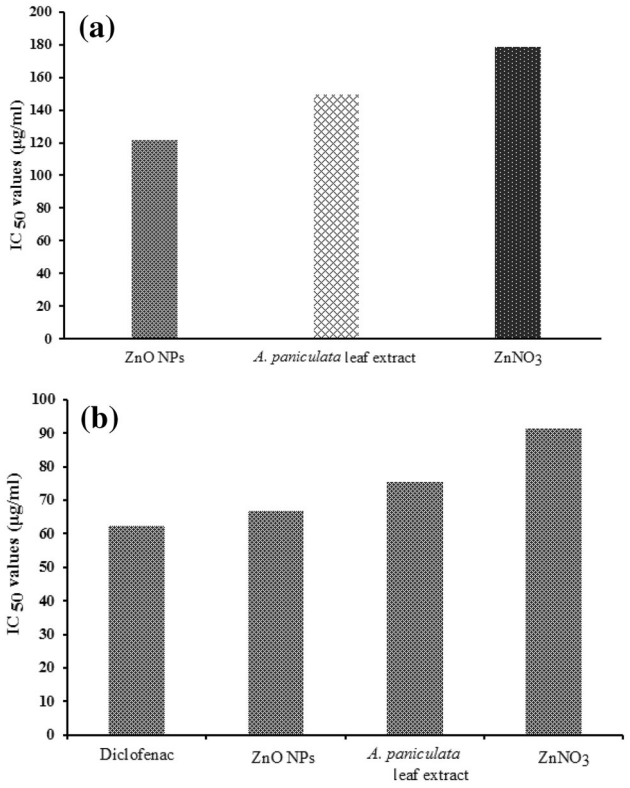

Fig. 6 Bio-potential of zinc oxide nanoparticles **a** anti-diabetic potential; **b** anti-inflammatory activity

IC_{50} value (Fig. 6b). Nagajyothi et al. [57] utilized the root extract of *Polygala tenuifolia* to synthesize the ZnO NPs and their antioxidants, as well as anti-inflammatory activity, were performed with the help of scavenging agent DPPH free radical assay and LPS-stimulated RAW 264.7 murine macrophages, respectively. To determine the biomedical potential of ZnO NPs, Thatoi et al. [58] fabricated the ZnO NPs using the aqueous extracts of two mangrove plants, viz. *Heritiera fomes* and *Sonneratia apetala* and revealed that the ZnO NPs have greater potential for anti-inflammation (79%) in comparison with silver nanoparticles (69.1%) and hence have potential to be utilized in the biomedical field.

Conclusion

In the present work, ZnO NPs were biosynthesis through green approach, inexpensive, pollution-free and eco-friendly approach for anti-oxidants, anti-diabetic and anti-inflammatory activity using *A. paniculata* extract. The synthesis of ZnO NPs was characterized using UV–Vis, FTIR, XRD, SEM, TEM and SAED analysis. The results proved the formation of ZnO NPs with distinguished spherical and hexagonal morphology. The particles obtained have been found to be predominantly spherical and the particle size could be controlled by varying the concentrations of leaf broth solution. The ZnO NPs were formed due to the influence of proteins and metabolites such as polyphenols, alkaloids carboxylic acid and flavonoids, especially due to the presence of free amino and carboxylic groups that have interacted with the zinc surface. Anti-oxidant, anti-diabetic and anti-inflammatory studies results proved that the synthesized ZnO NPs can be used to reduce the sugar level and to inflammations. Biosynthesized ZnO NPs prepared from *A. paniculata* are expected to have notable applications in pharmaceutical and biomedical fields such as drug delivery and in cosmetic industries.

Acknowledgements This paper was supported by the KU-Research Professor Program of Konkuk University, Seoul, South Korea.

Compliance with ethical standards

Conflict of interest The authors declare that they have no competing interests.

References

1. Gilaki M (2010) Biosynthesis of silver nanoparticles using plant extracts. J Biol Sci 10(5):465–467
2. Raveendran P, Fu J, Scott L (2003) Completely green synthesis and stabilization of metal nanoparticles. J Am Chem Soc 125:13940–13941
3. Sahu AN (2013) Nanotechnology in herbal medicines and cosmetics. Int Res Ayurveda Pharma 4(3):472–474
4. Ramesh P, Rajendran A, Meenakshisundaram M (2014) Green synthesis of zinc oxide nanoparticles using flower extract *Cassia Auriculata*. J Nanosci Nanotechnol 1(1):41–45
5. Rouhi J, Mahmud S, Naderi N, Ooi CR, Mahmood MR (2013) Physical properties of fish gelatin-based bio-nanocomposite films incorporated with ZnO nanorods. Nanoscale Res Lett 8:364
6. Mittal AK, Chisti Y, Banerjee UC (2013) Synthesis of metallic nanoparticles using plant extracts. Biotechnol Adv 31:346–356
7. Kairyte K, Kadys A, Luksiene Z (2013) Antibacterial and antifungal activity of photoactivated ZnO nanoparticles in suspension. J Photochem Photobiol B 128:78–84
8. Kajbafvala A, Ghorbani H, Paravar A, Samberg JP, Kajbafvala E, Sadrnezhaad SK (2012) Effects of morphology on photocatalytic performance of zinc oxide nanostructures synthesized by rapid microwave irradiation methods. Superlattices Microstruct 51(4):512–522
9. Kumar SS, Venkateswarlu P, Rao VR, Rao GN (2013) Synthesis, characterization and optical properties of zinc oxide nanoparticles. Int Nano Lett 3:30. doi:10.1186/2228-5326-3-30
10. Sundrarajan M, Ambika S, Bharathi K (2015) Plant extract mediated synthesis of ZnO nanoparticles using *Pongamia pinnata* and their activity against bacteria. Adv Powder Technol 26:1294–1299
11. Elumalai K, Velmurugan S, Ravi S, Kathiravan V, Adaikala Raj G (2015) Bio-approach: plant mediated synthesis of ZnO nanoparticles and their catalytic reduction of methylene blue and antimicrobial activity. Adv Powder Technol 26:1639–1651
12. Shekhawat MS, Ravindran CP, Manokari M (2015) A green approach to synthesize the zinc oxide nanoparticles using aqueous extracts of *Ficus benghalensis* L. Int J Biosci Agric Technol 6:1–5

13. Mishra V, Sharma R (2015) Green synthesis of zinc oxide nanoparticles using fresh peels extract of *Punica granatum* and its antimicrobial activities. Int J Pharma Res Health Sci 3:694–699
14. Dobrucka R, Dlugaszewska J (2016) Biosynthesis and antibacterial activity of ZnO nanoparticles using *Trifolium pratense* flower extract. Saudi J Bio Sci 23:517–523
15. Bala N, Saha S, Chakraborty M, Maiti M, Das S, Basu R, Nandy P (2015) Green synthesis of zinc oxide nanoparticles using *Hibiscus subdariffa* leaf extract: effect of temperature on synthesis, antibacterial activity and anti-diabetic activity. RSC Adv 5:4993–5003
16. Manokari M, Shekhawat MS (2016) Biogenesis of zinc oxide nanoparticles using *Couroupita guianensis* Aubl. extracts—a green approach. World Sci News 29:135–145
17. Akbar S (2011) *Andrographis paniculata:* a review of pharmacological activities and clinical effects. Alter Med Rev 16:66–77
18. Kabir MH, Hasan N, Rahman MM et al (2014) A survey of medicinal plants used by the Deb barma clan of the Tripura tribe of Moulvibazar district, Bangladesh. J Ethnobiol Ethnomed 10:19
19. Li W, Xu X, Zhang H et al (2007) Secondary metabolites from *Andrographis paniculata*. Chem Pharma Bull 55:455–458
20. Harjotaruno S, Widyawaruyantil A, Zaini NC (2008) Apoptosis inducing effect of andrographolide on TD-47 human breast cancer cell line. Afr J Tradit Complement 4:345–351
21. Gupta S, Yadava JNS, Tandon JS (1993) Antisecretory (antidiarrhoeal) activity of Indian medicinal plants against *Escherichia coli* enterotoxin-induced secretion in rabbit and guinea pig ileal loop models. Int J Pharma 31:198–204
22. Tang W, Eisenbrand G (1992) *Andrographis paniculata* (Burm. f.) Nees. In: Tang W, Eisenbrand G (eds) Chinese drugs of plant origin chemistry, pharmacology, and use in radiational and modern medicine. Springer, Berlin, pp 97–103
23. Nanduri S, Nyavanandi VK, Thunuguntla SSR et al (2004) Synthesis and structure–activity relationships of andrographolide analogues as novel cytotoxic agents. Bioorg Med Chem Lett 14:4711–4717
24. Subramanian R, Asmawi MZ, Sadikun A (2008) In vitro α-glucosidase and α-amylase enzyme inhibitory effects of *Andrographis paniculata* extract and andrographolide. Acta Biochim Polonica 55:391–398
25. Sheeja K, Shihab PK, Kuttan G (2006) Antioxidant and anti-inflammatory activities of the plant *Andrographis paniculata* nees. Immunopharmacol Immunotoxicol 28:129–140
26. Wiart C, Kumar K, Yusof MY, Hamimah H, Fauzi ZM, Sulaiman M (2005) Antiviral properties of ent-labdene diterpenes of *Andrographis paniculata* Nees, inhibitors of herpes simplex virus type 1. Phytother Res 19(12):1069–1070
27. Akowuah GA, Zhari I, Mariam A (2008) Analysis of urinary andrographolides and antioxidant status after oral administration of *Andrographis paniculata* leaf extract in rats. Food Chem Toxicol 46(12):3616–3620
28. Tan BKH, Zhang A (2004) *Andrographis paniculata* and the cardiovascular system. In: Packe L, Ong CN, Halliwell B (eds) Herbal and traditional medicine, biomolecular and clinical aspects, vol 14. CRC Press, Boca Raton, pp 441–456
29. Visen PKS, Saraswat B, Vuksan V, Dhawan BN (2007) Effect of andrographolide on monkey hepatocytes against galactosamine induced cell toxicity: an in vitro study. J Complement Integr Med 4:10
30. Iruretagoyen MI, Tobar JA, González PA et al (2005) Andrographolide interferes with T cell activation and reduces experimental autoimmune encephalomyelitis in the mouse. J Pharmacol Exp Ther 312(1):366–372
31. Akbarsha MA, Murugaian P (2000) Aspects of the male reproductive toxicity/male antifertility property of andrographolide in albino rats: effect on the testis and the cauda epididymidal spermatozoa. Phytother Res 14(6):432–435
32. Lin FL, Wu SJ, Lee SC, Ng LT (2009) Antioxidant, antioedema and analgesic activities of *Andrographis paniculata* extracts and their active constituent andrographolide. Phytother Res 23(7):958–964
33. Murali M, Mahendra C, Nagabhushan Rajashekar N, Sudarshana MS, Raveesha KA, Amruthesh KN (2017) Antibacterial and antioxidant properties of biosynthesized zinc oxide nanoparticles from *Ceropegia candelabrum* L.—an endemic species. Spectrochim Acta A Mol Biomol Spectrosc 15(179):104–109
34. Tran PD, Batabyal SK, Pramana SS, Barber J, Wong LH, Loo SCJ (2012) A cuprous oxide-reduced graphene oxide (Cu_2O–rGO) composite photocatalyst for hydrogen generation: employing rGO as an electron acceptor to enhance the photocatalytic activity and stability of Cu_2O. Nanoscale 4:3875–3878
35. Oyaizu M (1986) Studies on products of browning reactions: antioxidative activities of products of browning reaction prepared from glucosamine. Jpn J Nutr 44:307–315
36. Patel Rajesh M, Patel Natvar J (2011) In vitro antioxidant activity of coumarin compounds by DPPH, super oxide and nitric oxide free radical scavenging methods. J Adv Pharm Educ Res 1:52–68
37. Sekar N, Sangeetha R (2014) Amylase inhibitory potential of silver nanoparticles biosynthesized using *Breynia retusa* leaf extract. World J Pharma Res 3(7):1055–1066
38. Karthik K, Bharath R, Kumar P, Priya VR, Kumar SK, Rathore RSB (2013) Evaluation of anti-inflammatory activity of *Canthium parviflorum* by in vitro method. Ind J Res Pharm Biotechnol 1(5):729–731
39. Gupta A, Srivastava P, Bahadur L, Amalnerkar DP, Chauhan R (2015) Comparison of physical and electrochemical properties of ZnO prepared via different surfactant-assisted precipitation routes. Appl Nanosci 5:787–794
40. Oladiran AA, Olabisi IAM (2013) Synthesis and characterization of ZnO nanoparticles with zinc chloride as zinc source. Asian J Nat Appl Sci 2:41–44
41. Vimala K, Sundarraj S, Paulpandi M (2014) Green synthesized doxorubicin loaded zinc oxide nanoparticles regulates the Bax and Bcl-2 expression in breast and colon carcinoma. Process Biochem 49:160–172
42. Senthilkumar SR, Sivkumar T (2014) Green tea (*Camellia sinensis*) mediated synthesis of zinc oxide (ZnO) nanoparticles and studies on their antimicrobial activities. Int J Pharm Pharm Sci 6(6):461–465
43. Sangeetha G, Rajeshwari S, Venckatesh R (2011) Green synthesis of zinc oxide nanoparticles by *aloe barbadensis* miller leaf extract: structure and optical properties. Mater Res Bull 46:2560–2566
44. ShivShankar S, Ahmad A, Sastry M (2003) Geranium leaf assisted biosynthesis of silver nanoparticles. Biotechnol Prog 8:1627–1631
45. Tas AC, Majewski PJ, Aldinger F (2000) Chemical preparation of pure and strontium and/0r magnesium doped lanthanum gallata powders. J Am Ceram Soc 83(12):2954–2960
46. Wahab R, Ansari SG, KimYS Dar MA, Shin HS (2008) Synthesis and characterization of hydrozincite and its conversion into zinc oxide nanoparticles. J Alloys Compd 461:66–71 **(WHO 2014, malaria, fact sheet no. 94)**
47. Elumalai K, Velmurugan S (2015) Green synthesis, characterization and antimicrobial activities of zinc oxide nanoparticles from the leaf extract of *Azadirachta indica* (L.). Appl Surf Sci 345:329–336
48. Shah MA (2008) Formation of zinc oxide nanoparticles by the reaction of zinc metal with methanol at very low temperature. Afr Phys Rev 2:0011

49. Salam HA, Sivaraj R, Venckatesh R (2014) Green synthesis and characterization of zinc oxide nanoparticles from *Ocimum basilicum* L. var. purpurascens Benth.-Lamiaceae leaf extract. Mater Lett 131:16–18
50. Yun SW, Shin YJ, Cho SG (1998) Somteromg Behavior and Electrical Characteristics of ZnO Variators Prepared by Pechini Process. J Kor Ceram Soc 35(5):498
51. Ryu JH, Lim CS, Auh KH (2002) Synthesis of $ZnWO_4$ nanopowders by polymerized complex method. J Kor Ceram Soc 39(3):321
52. Vidhu VK, Philip D (2015) Biogenic synthesis of SnO_2 nanoparticles: evaluation of antibacterial and antioxidant activities. Spectrochim Acta A 134:372
53. Madan HR, Sharma SC, Dayabhanu U, Suresh D, Vidya YS et al (2015) Facile green fabrication of nanostructure ZnO plates, bullets, flower, prismatic tip, closed pine cone: their antibacterial, antioxidant, photo luminescent and photo catalytic properties. Spectrochim Acta Part A Mol Biomol Spectrosc 152:404–416
54. Singh BN, Rawat AK, Khan W, Naqvi AH, Singh BR (2014) Biosynthesis of stable antioxidant ZnO nanoparticles by *Pseudomonas aeruginosa* rhamnolipids. PLoS One 9:e106937
55. Halliwell B (1997) Antioxidants and human disease: a general introduction. Nutr Rev 55(1 Pt 2):S44–S49
56. Egefjord L, Petersen AB, Bak AM, Rungby J (2010) Zinc, alpha cells and glucagon secretion. Curr Diabetes Rev 6(1):52–57
57. Nagajyothi PC, Ju S, Jun I, Sreekanth TVM, Joong K, Mook H (2015) Biology antioxidant and anti-inflammatory activities of zinc oxide nanoparticles synthesized using *Polygala tenuifolia* root extract. J Photochem Photobiol B Biol 146:10–17
58. Thatoi P, Kerry RG, Gouda S, Das G et al (2016) Photo-mediated green synthesis of silver and zinc oxide nanoparticles using aqueous extracts of two mangrove plant species, *Heritiera fomes* and *Sonneratia apetala* and investigation of their biomedical applications. J Photochem Photobiol B Biol 163:311–318
59. Liu HL, Dai SA, Fu KY, Hsu SH (2010) Antibacterial properties of silver nanoparticles in three different sizes and their nanocomposites with a new waterborne polyurethane. Int J Nanomed 5:1017–1028